ChemComm

On-surface synthesis of super-heptazethrene

Journal:	*ChemComm*
Manuscript ID	CC-COM-04-2020-002513.R1
Article Type:	Communication

SCHOLARONE™
Manuscripts

Please do not adjust margins

COMMUNICATION

On-surface synthesis of super-heptazethrene†

Shantanu Mishra,‡[a] Jason Melidonie,‡[b] Kristjan Eimre,[a] Sebastian Obermann,[b] Oliver Gröning,[a] Carlo A. Pignedoli,[a] Pascal Ruffieux,[a] Xinliang Feng*[b] and Roman Fasel,*[ac]

Received 00th January 20xx,
Accepted 00th January 20xx

DOI: 10.1039/x0xx00000x

Zethrenes are model diradicaloids with potential applications in spintronics and optoelectronics. Despite a rich chemistry in solution, on-surface synthesis of zethrenes has never been demonstrated. We report the on-surface synthesis of super-heptazethrene on Au(111). Scanning tunneling spectroscopy investigations reveal that super-heptazethrene exhibits an exceedingly low HOMO-LUMO gap of 230 meV and, in contrast to its open-shell singlet ground state in the solution phase and in the solid-state, likely adopts a closed-shell ground state on Au(111).

Conjugated polycyclic hydrocarbons, or nanographenes (NGs), have emerged as an appealing class of materials with widely tunable properties that depend on their size, shape, and importantly, the structure of the edges. In particular, NGs with zigzag edges may display an open-shell ground state, which makes them highly attractive toward applications in molecular electronics and spintronics.[1] The synthesis of open-shell NGs in solution remains an enduring challenge due to their high reactivity, which, in most cases, requires thermodynamic and kinetic stabilization to obtain stable compounds. Prominent examples of open-shell NGs that have been synthesized in solution include anthenes,[2,3] periacenes,[4] zethrenes[5] and non-Kekulé frameworks based on phenalenyl radical[6,7] and triangulene.[8] Alternatively, on-surface synthesis[9] under ultrahigh vacuum represents a promising route to achieve open-shell NGs, and offers the possibility of conducting atomic-scale structural and electronic characterization of individual molecules using scanning tunneling microscopy (STM) and spectroscopy (STS). In the past few years, elusive open-shell NGs such as triangulene and its π-extended homologues,[10–12] Clar's goblet[13] and zigzag graphene nanoribbons[14] have been synthesized on metal and insulator surfaces, opening unique opportunities to study all-carbon magnetism at the nanoscale.

The family of zethrenes, which constitute Z-shaped NGs containing mixed zigzag/armchair edges (Fig. 1a), have received increasing attention as diradicaloids. While the parent zethrene, incorporating a 1,3-butadiene moiety in the molecular framework, is a closed-shell compound,[15] longitudinal extension of zethrenes generates proaromatic quinodimethane moieties at the molecular core, which endows moderate diradical character to these compounds.[16,17] Notably, the open-shell character of zethrenes is shown to significantly increase through lateral extension, which gives rise to the so-called super-zethrene compounds.[18,19] Over the past years, the development of zethrene chemistry in solution has served to highlight the potential of these compounds as near-infrared dyes, nonlinear optical chromophores and charge transport materials.[5] On the other hand, the synthesis of zethrenes has remained an unexplored topic in surface chemistry, in contrast to related NGs such as acenes,[20–22] periacenes[23,24] and anthenes,[25] which have been extensively studied on surfaces. Here, we report the first on-surface synthesis of a zethrene compound, super-heptazethrene (**1**, Fig. 1b), on Au(111), and its detailed electronic characterization by STS, supported by tight-binding (TB), mean-field Hubbard (MFH), density functional theory (DFT) and many-body perturbation theory GW calculations.

The synthesis of **1** is based on the precursor 9,9'-(2,6-dimethylnaphthalene-1,5-diyl)dianthracene (**2**), which is expected to undergo thermally induced cyclodehydrogenation and oxidative cyclization of methyl groups on a metal surface (Fig. 1b). The synthesis of **2** was performed starting from the treatment of 2,6-dimethylnaphthalene (**3**) with a slight excess of bromine, which provided 1,5-dibromo-2,6-dimethylnaphthalene (**4**) in excellent yield.[26] In a next step, 2,2'-(2,6-dimethylnaphthalene-1,5-diyl)bis(4,4,5,5-tetramethyl-1,3,2-dioxaborolane) (**5**) was obtained by Suzuki-Miyaura conditions in 33% yield using [1,1'-

[a] Empa—Swiss Federal Laboratories for Materials Science and Technology, Überlandstrasse 129, 8600 Dübendorf, Switzerland.
[b] Faculty of Chemistry and Food Chemistry, and Center for Advancing Electronics Dresden, Technical University of Dresden, 01062 Dresden, Germany.
[c] Department of Chemistry and Biochemistry, University of Bern, Freiestrasse 3, 3012 Bern, Switzerland.

† Electronic Supplementary Information (ESI) available. See DOI: 10.1039/x0xx00000x

‡ These authors contributed equally to this work.

Please do not adjust margins

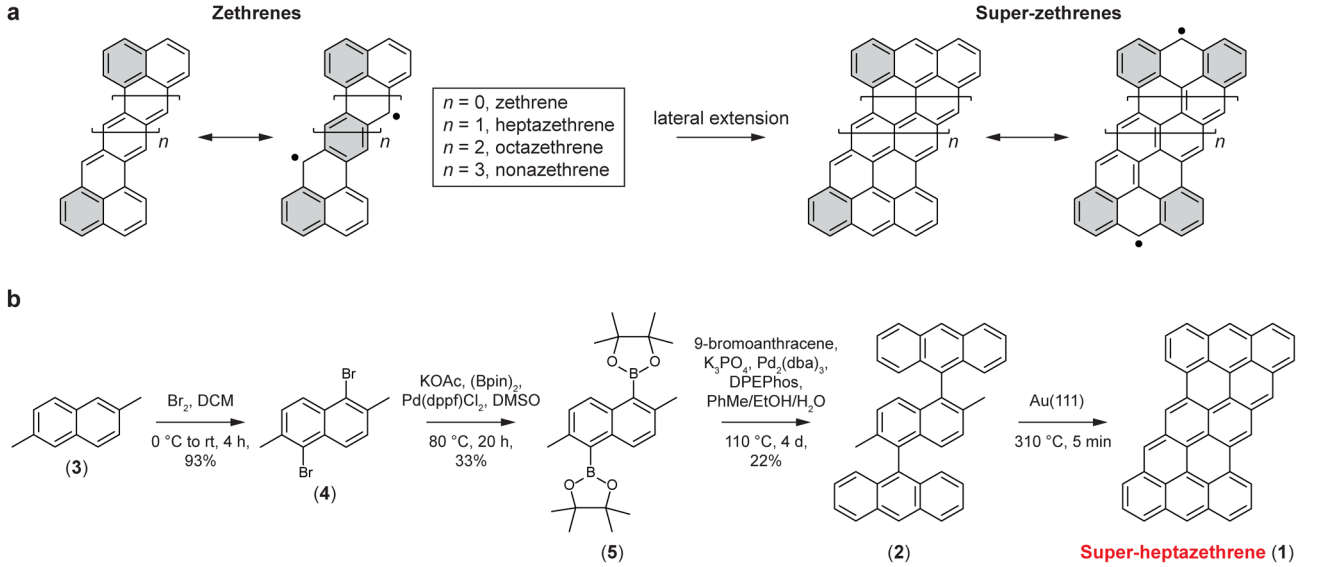

Fig. 1 (a) Schematic illustration of the closed-shell Kekulé and open-shell non-Kekulé resonance structures of zethrenes and super-zethrenes. (b) Combined in-solution and on-surface synthetic route toward **1**.

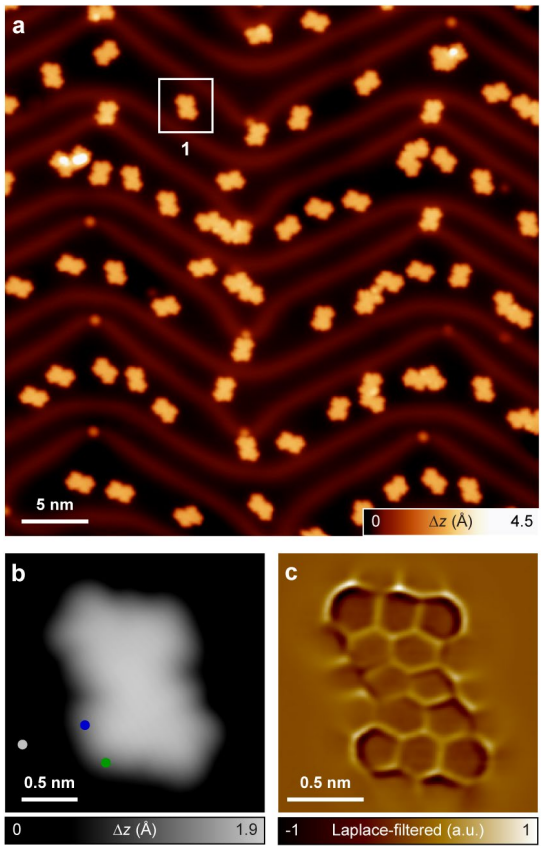

Fig. 2 On-surface synthesis and structural characterization of **1**. (a) Overview STM image after annealing **2** on Au(111) at 310 °C. An individual super-heptazethrene molecule is highlighted with a square. (b) High-resolution STM image of **1** acquired with a CO-functionalized tip. The colored dots indicate the locations at which the d*I*/d*V* spectra shown in Fig. 3a were acquired. (c) Corresponding Laplace-filtered ultrahigh-resolution STM image of **1**, showing the bond-resolved structure. Scanning parameters: (a) $V = -1.2$ V, $I = 100$ pA; (b) $V = -100$ mV, $I = 50$ pA; (c) $V = -5$ mV, $I = 50$ pA, $\Delta z = -0.7$ Å.

bis(diphenylphosphino)ferrocene]dichloropalladium(II) as the catalyst, potassium acetate as the base and bis(pinacolato)diboron ($(Bpin)_2$) as the borylation reagent.[27] Finally, anthracene substituents were introduced to **5** through the Suzuki reaction, leading to the formation of **2** in 22% yield under the catalysis of tris(dibenzylideneacetone)dipalladium(0) ($Pd_2(dba)_3$) and bis[(2-diphenylphosphino)phenyl] ether (DPEPhos).[28] Subsequently, **2** was sublimed on a Au(111) surface held at room temperature and annealed to 310 °C to promote the on-surface reactions. Fig. 2a presents an overview STM image of the surface after the annealing step, revealing the predominance of isolated molecules, along with a minority of oligomers resulting from intermolecular coupling reactions. Fig. 2b and c show high-resolution and ultrahigh-resolution[29,30] STM images, respectively, of an individual molecule, which confirm the successful formation of **1** (also see Fig. S1, ESI†). The on-surface yield of **1** amounts to 82%.

We probed the electronic structure of **1** at submolecular resolution through STS. d*I*/d*V* spectroscopy on **1** presents reproducible spectral features at −1.05 V, −110 mV, +120 mV and +1.70 V (Fig. 3a), which we tentatively assign to the HOMO−1, HOMO, LUMO and LUMO+1 resonances of **1**, respectively (HOMO and LUMO refer to the highest occupied and lowest unoccupied molecular orbitals). Therefore, **1** on Au(111) exhibits a remarkably small HOMO-LUMO gap of 230 meV. The magnetic ground state of super-zethrenes is reported to be open-shell both in the solution and in the solid-state. In particular, the study of a super-heptazethrene derivative by Zeng et al.[18] concluded that the compound exhibits an open-shell singlet ground state with a singlet-triplet gap of approximately 41 meV. To investigate the magnetic ground state of **1** on Au(111), our starting point is the electronic structure calculation of **1** within the nearest neighbor TB model, which disregards electron-electron interactions necessary to describe magnetism and thus leads to a closed-shell state. The salient feature in the TB energy spectrum of **1** (Fig. 3c) corresponds to a pair of frontier states located close to zero energy, which conform to the fully occupied HOMO and the empty LUMO (see Fig. S2, ESI† for the calculated orbital wave

This journal is © The Royal Society of Chemistry 2020

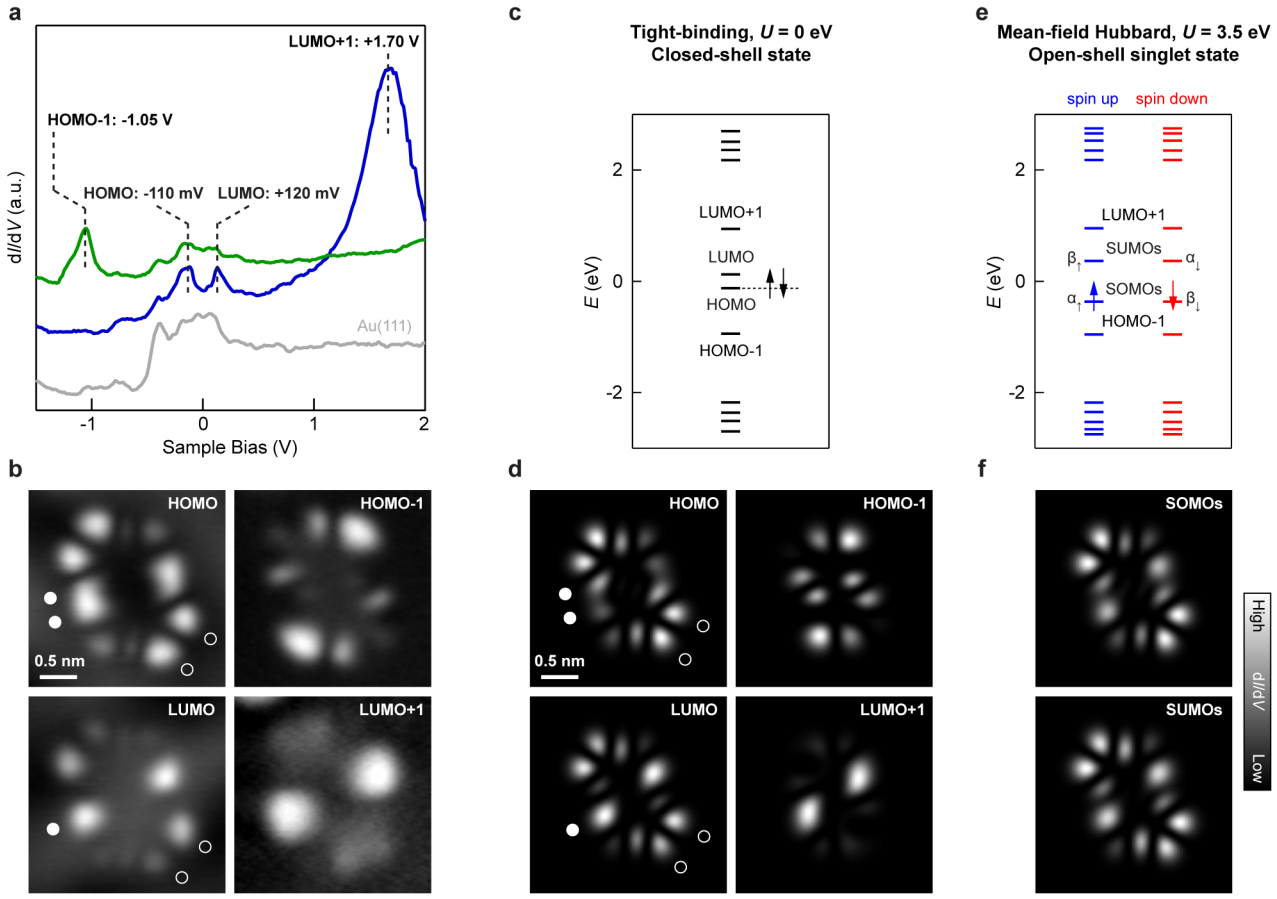

Fig. 3 Electronic characterization of **1**. (a) d*I*/d*V* spectroscopy on **1** revealing molecular orbital resonances. Acquisition positions for the spectra are highlighted in Fig. 2b. (b) Constant-current d*I*/d*V* maps acquired at the resonances indicated in (a) (I = 300 pA, V_{rms} = 24 mV). (c and d) TB energy spectrum (c), along with the HOMO−1 to LUMO+1 TB-LDOS maps (d) of **1**. (e and f) MFH energy spectrum (e), along with the SOMOs and SUMOs MFH-LDOS maps (f) of **1**. U denotes the on-site Coulomb repulsion. Open feedback parameters for d*I*/d*V* spectroscopy: V = −1.5 V, I = 350 pA; V_{rms} = 14 mV.

functions). Next, we employ the MFH model to describe electron-electron interactions in **1**, which leads to spin polarization of the system. The frontier electronic structure is now characterized by a pair of singly occupied molecular orbitals (SOMOs, Fig. 3e) α and β, with an antiferromagnetic alignment of the populating spins—that is, an open-shell singlet ground state (see Fig. S3 and S4, ESI† for the MFH and DFT energetics of the open-shell singlet and triplet states of **1**). In this scenario, the spin up and spin down channels of the α and β orbitals, respectively, are occupied by one electron each, with the corresponding spin down and spin up channels empty (labeled as SUMOs in Fig. 3e, where SUMOs stands for singly unoccupied molecular orbitals) and separated from the occupied spin channels by a Coulomb gap. The calculated spin-polarized wave functions of α and β exhibit a largely disjoint character, being sublattice-polarized and localized at the opposite ends of **1** (Fig. S2, ESI†). Fig. 3b presents the spatially-resolved constant-current d*I*/d*V* maps at the HOMO−1, HOMO, LUMO and LUMO+1 resonances of **1**, which reveal the probability densities of the respective orbital wave functions (also see Fig. S5, ESI† for constant-height d*I*/d*V* maps). Importantly, the frontier orbital d*I*/d*V* maps present two notable differences: (1) as highlighted by the filled circles, the HOMO map reveals two prominent lobes of roughly equal intensity along the long molecular axis, while the LUMO map presents only one lobe at this location, and (2) as highlighted by the empty circles, and in contrast to the HOMO map, the LUMO map presents a notable difference in intensity between the two lobes at the molecular termini. To link the aforementioned LDOS features in the d*I*/d*V* maps to the open- or closed-shell ground state of **1** on Au(111), we simulated the LDOS maps of the frontier orbitals of **1** both for the closed-shell (TB model) and the open-shell singlet (MFH model) configurations, as shown in Fig. 3d and f, respectively. The experimental d*I*/d*V* maps of the frontier orbitals clearly concur with the TB-LDOS maps of the HOMO and LUMO of **1**, which supports a closed-shell ground state of **1** on Au(111). In the case of an open-shell singlet ground state, the frontier orbital maps should exhibit similar appearances since tunneling of electrons to/from the same orbitals are involved.[13,31] It is to be noted that in the present case, the SOMOs and SUMOs MFH-LDOS maps (Fig. 3f), while exhibiting similar shapes and symmetries, present minor differences, which arise due to a finite hybridization energy in **1** (evidenced by a finite TB gap). To further probe the magnetic ground state of **1** on Au(111), we performed GW calculations including screening effects from the underlying surface (GW+IC calculations; Fig. S4, ESI†). Our calculations reveal that the experimental gap of 230 meV of **1** on Au(111) reasonably agrees

with the GW+IC gap of 120 meV for the closed-shell state of **1**, and substantially differs from the GW+IC gap of 1.14 eV for the open-shell singlet state of **1**, which further supports a closed-shell ground state of **1** on Au(111). Finally, previous studies of open-shell singlet NGs on surfaces have demonstrated inelastic singlet-triplet spin excitations,[13,32,33] which are, however, absent in the present case, in accordance with a closed-shell ground state of **1**.

In conclusion, we have demonstrated the on-surface synthesis of super-heptazethrene on Au(111) with excellent yields. The molecule exhibits a very small HOMO-LUMO gap of 230 meV on Au(111). Comparison of STS data with extensive mean-field and many-body perturbation theory calculations supports that super-heptazethrene exhibits a closed-shell ground state on Au(111). Our synthetic methodology renders new opportunities toward atomic-scale exploration of larger zethrenes as probable candidate molecules exhibiting all-carbon magnetism.

This work was supported by the Swiss National Science Foundation (grant nos. 200020-182015 and IZLCZ2-170184), the EU Horizon 2020 research and innovation program – Marie Skłodowska-Curie grant no. 813036 and Graphene Flagship Core 2 (grant no. 785219), the Office of Naval Research (grant no. N00014-18-1-2708), ERC Consolidator grant (T2DCP, no. 819698), the German Research Foundation within the Cluster of Excellence – Center for Advancing Electronics Dresden and EnhanceNano (grant no. 391979941), the European Social Fund and the Federal State of Saxony (ESF-Project GRAPHD, TU Dresden) and CSCS (project ID 904).

Conflicts of interest

There are no conflicts to declare.

References

1 S. Das and J. Wu, *Phys. Sci. Rev.*, 2017, **2**, 109.
2 A. Konishi, Y. Hirao, M. Nakano, A. Shimizu, E. Botek, B. Champagne, D. Shiomi, K. Sato, T. Takui, K. Matsumoto, H. Kurata and T. Kubo, *J. Am. Chem. Soc.*, 2010, **132**, 11021–11023.
3 A. Konishi, Y. Hirao, K. Matsumoto, H. Kurata, R. Kishi, Y. Shigeta, M. Nakano, K. Tokunaga, K. Kamada and T. Kubo, *J. Am. Chem. Soc.*, 2013, **135**, 1430–1437.
4 M. R. Ajayakumar, Y. Fu, J. Ma, F. Hennersdorf, H. Komber, J. J. Weigand, A. Alfonsov, A. A. Popov, R. Berger, J. Liu, K. Müllen and X. Feng, *J. Am. Chem. Soc.*, 2018, **140**, 6240–6244.
5 P. Hu and J. Wu, *Can. J. Chem.*, 2016, **95**, 223–233.
6 K. Goto, T. Kubo, K. Yamamoto, K. Nakasuji, K. Sato, D. Shiomi, T. Takui, M. Kubota, T. Kobayashi, K. Yakusi and J. Ouyang, *J. Am. Chem. Soc.*, 1999, **121**, 1619–1620.
7 Y. Li, K.-W. Huang, Z. Sun, R. D. Webster, Z. Zeng, W. Zeng, C. Chi, K. Furukawa and J. Wu, *Chem. Sci.*, 2014, **5**, 1908–1914.
8 J. Inoue, K. Fukui, T. Kubo, S. Nakazawa, K. Sato, D. Shiomi, Y. Morita, K. Yamamoto, T. Takui and K. Nakasuji, *J. Am. Chem. Soc.*, 2001, **123**, 12702–12703.
9 S. Clair and D. G. de Oteyza, *Chem. Rev.*, 2019, **119**, 4717–4776.
10 N. Pavliček, A. Mistry, Z. Majzik, N. Moll, G. Meyer, D. J. Fox and L. Gross, *Nat. Nanotechnol.*, 2017, **12**, 308–311.
11 S. Mishra, D. Beyer, K. Eimre, J. Liu, R. Berger, O. Gröning, C. A. Pignedoli, K. Müllen, R. Fasel, X. Feng and P. Ruffieux, *J. Am. Chem. Soc.*, 2019, **141**, 10621–10625.
12 J. Su, M. Telychko, P. Hu, G. Macam, P. Mutombo, H. Zhang, Y. Bao, F. Cheng, Z.-Q. Huang, Z. Qiu, S. J. R. Tan, H. Lin, P. Jelínek, F.-C. Chuang, J. Wu and J. Lu, *Sci. Adv.*, 2019, **5**, eaav7717.
13 S. Mishra, D. Beyer, K. Eimre, S. Kezilebieke, R. Berger, O. Gröning, C. A. Pignedoli, K. Müllen, P. Liljeroth, P. Ruffieux, X. Feng and R. Fasel, *Nat. Nanotechnol.*, 2020, **15**, 22–28.
14 P. Ruffieux, S. Wang, B. Yang, C. Sánchez-Sánchez, J. Liu, T. Dienel, L. Talirz, P. Shinde, C. A. Pignedoli, D. Passerone, T. Dumslaff, X. Feng, K. Müllen and R. Fasel, *Nature*, 2016, **531**, 489–492.
15 E. Clar, K. F. Lang and H. Schulz-Kiesow, *Chem. Ber.*, 1955, **88**, 1520–1527.
16 Y. Li, W.-K. Heng, B. S. Lee, N. Aratani, J. L. Zafra, N. Bao, R. Lee, Y. M. Sung, Z. Sun, K.-W. Huang, R. D. Webster, J. T. López Navarrete, D. Kim, A. Osuka, J. Casado, J. Ding and J. Wu, *J. Am. Chem. Soc.*, 2012, **134**, 14913–14922.
17 R. Huang, H. Phan, T. S. Herng, P. Hu, W. Zeng, S. Dong, S. Das, Y. Shen, J. Ding, D. Casanova and J. Wu, *J. Am. Chem. Soc.*, 2016, **138**, 10323–10330.
18 W. Zeng, Z. Sun, T. S. Herng, T. P. Gonçalves, T. Y. Gopalakrishna, K.-W. Huang, J. Ding and J. Wu, *Angew. Chem. Int. Ed.*, 2016, **55**, 8615–8619.
19 W. Zeng, T. Y. Gopalakrishna, H. Phan, T. Tanaka, T. S. Herng, J. Ding, A. Osuka and J. Wu, *J. Am. Chem. Soc.*, 2018, **140**, 14054–14058.
20 J. I. Urgel, S. Mishra, H. Hayashi, J. Wilhelm, C. A. Pignedoli, M. D. Giovannantonio, R. Widmer, M. Yamashita, N. Hieda, P. Ruffieux, H. Yamada and R. Fasel, *Nat. Commun.*, 2019, **10**, 861.
21 R. Zuzak, R. Dorel, M. Kolmer, M. Szymonski, S. Godlewski and A. M. Echavarren, *Angew. Chem. Int. Ed.*, 2018, **57**, 10500–10505.
22 F. Eisenhut, T. Kühne, F. García, S. Fernández, E. Guitián, D. Pérez, G. Trinquier, G. Cuniberti, C. Joachim, D. Peña and F. Moresco, *ACS Nano*, 2020, **14**, 1011–1017.
23 S. Mishra, T. G. Lohr, C. A. Pignedoli, J. Liu, R. Berger, J. I. Urgel, K. Müllen, X. Feng, P. Ruffieux and R. Fasel, *ACS Nano*, 2018, **12**, 11917–11927.
24 C. Rogers, C. Chen, Z. Pedramrazi, A. A. Omrani, H.-Z. Tsai, H. S. Jung, S. Lin, M. F. Crommie and F. R. Fischer, *Angew. Chem. Int. Ed.*, 2015, **54**, 15143–15146.
25 S. Wang, L. Talirz, C. A. Pignedoli, X. Feng, K. Müllen, R. Fasel and P. Ruffieux, *Nat. Commun.*, 2016, **7**, 11507.
26 K. Liu, F. Qiu, C. Yang, R. Tang, Y. Fu, S. Han, X. Zhuang, Y. Mai, F. Zhang and X. Feng, *Cryst. Growth Des.*, 2015, **15**, 3332–3338.
27 K. Xu, Y. Fu, Y. Zhou, F. Hennersdorf, P. Machata, I. Vincon, J. J. Weigand, A. A. Popov, R. Berger and X. Feng, *Angew. Chem. Int. Ed.*, 2017, **56**, 15876–15881.
28 Y. Gu, X. Wu, T. Y. Gopalakrishna, H. Phan and J. Wu, *Angew. Chem. Int. Ed.*, 2018, **57**, 6541–6545.
29 R. Temirov, S. Soubatch, O. Neucheva, A. C. Lassise and F. S. Tautz, *New J. Phys.*, 2008, **10**, 053012.
30 L. Gross, F. Mohn, N. Moll, P. Liljeroth and G. Meyer, *Science*, 2009, **325**, 1110–1114.
31 J. Repp, G. Meyer, S. Paavilainen, F. E. Olsson and M. Persson, *Science*, 2006, **312**, 1196–1199.
32 J. Li, S. Sanz, M. Corso, D. J. Choi, D. Peña, T. Frederiksen and J. I. Pascual, *Nat. Commun.*, 2019, **10**, 200.
33 S. Mishra, D. Beyer, K. Eimre, R. Ortiz, J. Fernández-Rossier, R. Berger, O. Gröning, C. Pignedoli, R. Fasel, X. Feng and P. Ruffieux, *Angew. Chem. Int. Ed.*, 2020, DOI: 10.1002/anie.202002687.

 This journal is © The Royal Society of Chemistry 2020

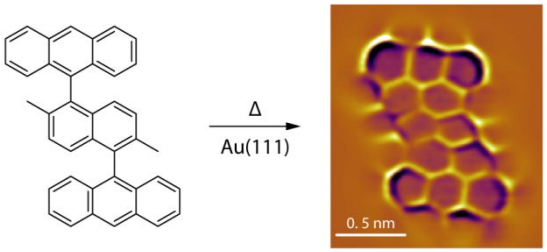

On-surface synthesis of a zethrene compound, super-heptazethrene, is reported on Au(111), along with its detailed characterization using scanning tunneling microscopy.